Biological Psychiatry: CNNI

Archival Report

Transdiagnostic Multimodal Neuroimaging in Psychosis: Structural, Resting-State, and Task Magnetic Resonance Imaging Correlates of Cognitive Control

Dov B. Lerman-Sinkoff, Sridhar Kandala, Vince D. Calhoun, Deanna M. Barch, and Daniel T. Mamah

ABSTRACT

BACKGROUND: Disorders with psychotic features, including schizophrenia and some bipolar disorders, are associated with impairments in regulation of goal-directed behavior, termed cognitive control. Cognitive control–related neural alterations have been studied in psychosis. However, studies are typically unimodal, and relationships across modalities of brain function and structure remain unclear. Thus, we performed transdiagnostic multimodal analyses to examine cognitive control–related neural variation in psychosis.

METHODS: Structural, resting, and working memory task imaging for 31 control participants, 27 participants with bipolar disorder, and 23 participants with schizophrenia were collected and processed identically to the Human Connectome Project, enabling identification of relationships with prior multimodal work. Two cognitive control–related independent components (ICs) derived from the Human Connectome Project using multiset canonical correlation analysis with joint IC analysis were used to predict performance in psychosis. De novo multiset canonical correlation analysis with joint IC analysis was performed, and the results were correlated with cognitive control.

RESULTS: A priori working memory and cortical thickness maps significantly predicted cognitive control in psychosis. De novo multiset canonical correlation analysis with joint IC analysis identified an IC correlated with cognitive control that also discriminated groups. Structural contributions included insular and cingulate regions; task contributions included precentral, posterior parietal, cingulate, and visual regions; and resting-state contributions highlighted canonical network organization. Follow-up analyses suggested that correlations with cognitive control were primarily influenced by participants with schizophrenia.

CONCLUSIONS: A priori and de novo imaging replicably identified a set of interrelated patterns across modalities and the healthy-to-psychosis spectrum, suggesting robustness of these features. Relationships between imaging and cognitive control performance suggest that shared symptomatology may be key to identifying transdiagnostic relationships in psychosis.

Keywords: Bipolar disorder, Cognitive control, mCCA+jICA, Multimodal fusion, Schizophrenia, Transdiagnostic psychosis

https://doi.org/10.1016/j.bpsc.2019.05.004

Psychosis, classically a hallmark of schizophrenia (1), is present in several other disorders including schizoaffective disorder and bipolar disorder (BD). Importantly, alterations in cognition (2–4), including cognitive control (5,6), are a key feature of psychosis. Furthermore, cognitive control alterations are observed transdiagnostically (7), including in individuals with schizophrenia and schizoaffective disorder (hereafter collectively referred to as SZ), BD (8), and other disorders (9–11). Here, we expand beyond prior work by using multimodal image analysis to examine transdiagnostic patterns of neural variation in structural, resting-state, and task imaging related to cognitive control.

Within the broad construct of cognition (12), cognitive control (13,14) refers to the set of cognitive functions that enable and support goal-directed behavior and regulation of one's thoughts and actions (15), including the ability to maintain information over time (e.g., working memory), protect against distraction, and combine novel inputs to provide flexibility in task execution (15,16). Evidence in psychosis suggests that task flexibility (17) may be the source of generalized neurocognitive deficit in SZ and possibly BD (4). Within the psychosis spectrum, participants with SZ have poorer cognitive control performance than healthy control participants (HC) do, and participants with BD often have intermediary performance between that of participants with SZ and that of HC (7,18,19). This graded performance further supports conceptualizations of psychosis as a dimensional transdiagnostic construct.

The imaging literature has identified transdiagnostic neural alterations in psychosis related to cognitive control. For example, with structural imaging, working memory performance was inversely correlated with cortical thickness in the right rostral anterior cingulate and positively correlated with surface area in the left rostral anterior cingulate and right rostral middle frontal region in a cohort of individuals with SZ and BD (20). Recent meta-analysis of structural alterations in a broad mental illness sample identified significant psychosis-related gray matter losses in medial prefrontal cortex (PFC), insula, thalamus, and amygdala and significant gray matter increases in the striatum compared with gray matter in HC and participants with nonpsychotic mental illnesses (21). Finally, Shepherd *et al.* (22) examined a transdiagnostic psychosis cohort and dichotomized patients into high and low executive function groups based on 2-back working memory performance. Compared with HC, the low executive function group exhibited decreased gray matter volume in bilateral superior and medial frontal gyri and right inferior operculum and hippocampus.

Resting-state imaging has also identified transdiagnostic neural alterations (23,24) related to general cognition (25–27), with fewer studies examining cognitive control (28). For example, trail-making task performance in persons with SZ and BD positively correlated with average connectivity strength between the whole brain and left caudate, thalamus, temporal occipital fusiform cortex, and lingual gyrus (25). Furthermore, a network connectivity approach in another transdiagnostic cohort (26) identified a significant relationship between global efficiency of the cingulo-opercular network and cognitive and executive function, along with significant decreases in cingulo-opercular network efficiency in psychosis (26). Additionally, an independent component analysis (ICA) approach to resting-state data (27) identified significant decreases in connectivity between a fronto-occipital component and a combined anterior default mode and prefrontal component in individuals with SZ or psychotic BD and unaffected siblings. In the same study, decreased connectivity was also identified between mesolimbic and paralimbic as well as sensory and motor components, but this was only observed in individuals with SZ and not in those with psychotic BD. Furthermore, recent analyses from the same dataset identified 7 abnormal networks exhibiting significant correlations with cognitive control including visual, working memory, visuomotor integration, default mode, and frontoparietal control networks (28).

Several studies have examined transdiagnostic alterations in task imaging related to cognitive control. For example, Brandt *et al.* (29) used ICA decompositions of 2-back working memory task and identified 9 task-related components. Of those, 3 components with spatial distribution in frontal and parietal regions corresponding to working memory networks showed significant graded hyperactivation pattern (SZ > BD > HC). Additionally, Smucny *et al.* (7) used an a priori contrast approach examining activation in dorsolateral PFC and superior parietal cortex during the AX-Continuous Performance Task in a transdiagnostic population. They identified significant graded task performance (HC>BD>SZ) and blood oxygen level–dependent responses in dorsolateral PFC and partially significant responses in superior parietal cortex.

As noted, a number of studies have examined neural alterations in psychosis. However, much of this literature is unimodal [see (30) for review and fuller motivation for multimodal imaging]. Thus, it remains unclear how extant results relate across modalities and across disease states. For example, are the same participants with structural correlates of poor cognitive control performance also the same participants exhibiting resting-state correlates of cognitive control performance? Multimodal analyses examining structural, resting-state, and diffusion imaging and relationships to a cognitive battery in SZ identified a relationship between overall cognitive impairment and variation in corticostriatothalamic circuitry (31). Additionally, examination of 3 modalities derived from structural imaging in a transdiagnostic cohort (HC, BD, and SZ) identified putative associations between gray matter alterations and processing speed, working memory, and attention (32). However, these associations were not significant across multiple diagnostic categories within the same component and did not survive multiple comparison correction. Importantly, both studies did not focus specifically on cognitive control.

We recently used multiset canonical correlation analysis with joint ICA (mCCA+jICA) to study multimodal neural correlates of cognitive control in the normative population (33). The mCCA+jICA framework was chosen as it flexibly identifies patterns across modalities and decomposes them into maximally spatially independent sources of variance (34). This has proven to be a powerful analytic framework and has been used to identify abnormalities in participants with SZ (35) and also to discriminate among HC and participants with BD and SZ (36). Using a community sample from the Human Connectome Project (HCP) (37), we identified relationships between 2 mCCA+jICA-derived multimodal patterns and individual differences in cognitive control performance (33). These 2 components included structural and functional contributions from the anterior insula, visual, and parietal regions as well canonical resting-state network structures. Importantly, the findings were replicable in an independent sample of participants from the HCP using both predictive and independent analyses.

The goal of the present study was to examine transdiagnostic multimodal neural alterations in psychosis, using the results of our previous work to guide analyses. To accomplish this, we recruited a transdiagnostic psychosis cohort composed of HC and participants with SZ and BD. Participants were imaged using the same HCP-customized scanner and performed a subset of the same HCP tasks. We first assessed the replicability of our normative findings by predicting performance in the psychosis participants using the 2 components from our prior work that were significantly related to cognitive control. We then performed an independent mCCA+jICA decomposition of this new transdiagnostic dataset to identify novel patterns of alteration.

METHODS AND MATERIALS

Participants

Participants were recruited from a broader study of neural alterations in psychosis and included HC, participants with SZ, and participants with BD. Prior to image preprocessing, there were 35 HC, 36 participants with BD, and 31 participants with SZ available. Of this, 31 HC (ultimately, n = 30;

Table 1. Demographics, Clinical Symptoms, and Behavioral Performance

	HC	BD	SZ	Omnibus Test Statistic	*p* Values
Age, Years	24.6 ± 3.1 (30)	26.7 ± 3.0 (27)	24.9 ± 3.7 (23)	$F_{2,77}$ = 3.21	Omnibus: .046
					HC vs. SZ: .943
					HC vs. BD: .049
					BD vs. SZ: .145
Gender	14 F, 16 M	13 F, 13 M	4 F, 18 M	χ^2 = 6.034	Omnibus: .197
Ethnicity, % Caucasian	57	80	29	χ^2 = 0.006	Omnibus: .002
					HC vs. SZ: .047
					HC vs. BD: .066
					BD vs. SZ: <.000
Education, Years	16.2 ± 2.4 (30)	15.3 ± 2.3 (26)	13.0 ± 1.4 (22)	$F_{2,75}$ = 14.9	Omnibus: <.000
					HC vs. SZ: <.000
					HC vs. BD: .264
					BD vs. SZ: .001
Parental Level of Education[a]	2.04 ± 1.3 (27)	2.28 ± 1.3 (25)	2.76 ± 1.1 (17)	$F_{2,66}$ = 1.71	Omnibus: .189
SAPS	0.1 ± 0.7 (30)	2.1 ± 2.9 (27)	4.6 ± 3.2 (23)	$F_{2,77}$ = 21.03	Omnibus: <.000
					HC vs. SZ: <.000
					HC vs. BD: .008
					BD vs. SZ: .003
SANS	0.8 ± 1.7 (29)	3.3 ± 3.5 (27)	6.3 ± 3.0 (23)	$F_{2,76}$ = 24.67	Omnibus: <.000
					HC vs. SZ: <.000
					HC vs. BD: .003
					BD vs. SZ: .002
WERCAP Psychosis History	0.90 ± 3.2 (30)	8.78 ± 7.4 (27)	31.83 ± 11.59 (23)	$F_{2,77}$ = 106.76	Omnibus: <.000
					HC vs. SZ: <.000
					HC vs. BD: .001
					BD vs. SZ: <.000
Cognitive Control Composite	0.40 ± 0.46 (30)	0.16 ± 0.58 (27)	−0.36 ± 0.85 (23)	$F_{2,77}$ = 9.579	Omnibus: <.000
					HC vs. SZ: <.000
					HC vs. BD: .332
					BD vs. SZ: .013

Values represent mean ± SD (*n*). The *n* values vary slightly owing to missing data. Tukey post hoc tests used to assess for differences across groups.

BD, participants with bipolar disorder; F, female; HC, healthy control participants; M, male; SANS, Scale for the Assessment of Negative Symptoms; SAPS, Scale for the Assessment of Positive Symptoms; SES, socioeconomic status; SZ, participants with schizophrenia and schizoaffective disorder; WERCAP, Washington Early Recognition Center Affectivity and Psychosis screen.

[a]Level of education scale: 1 = graduate professional training; 2 = completed undergraduate; 3 = partial college; 4 = high school graduate; 5 = partial high school; 6 = junior high school; 7 = less than 7 years of education.

see the Supplement for details) and 27 participants with BD and 23 with SZ had the requisite data for inclusion in this study. Participants were recruited from clinical and community settings in Saint Louis. Participants had no substance use disorder in the previous 6 months, no clinically significant head trauma, and no neurological diseases. Patient participation criteria included DSM-IV diagnosis of BD or SZ, age 18 to 30 years, and stable outpatient or partial hospital status. HC were recruited to have similar demographics (age, gender, parental level of education) as patients. HC participation criteria included no history of DSM-IV psychotic disorder and no cognitive enhancing or psychotropic medication for the previous 3 months. Study procedures were approved by the Washington University in St. Louis Institutional Review Board, and all participants gave written informed consent.

Behavioral Assessment

A composite measure of cognitive control was generated for each participant from their performance on 4 tasks (see the Supplement for details on each task): 1) in-scanner *n*-back task; 2) out-of-scanner letter *n*-back task from the Penn Computerized Neuropsychological battery (38); 3) progressive matrices from the Penn Computerized Neuropsychological battery; and 4) Penn Conditional Exclusion Task accuracy. Performance on each task was individually *Z*-scored and averaged to generate the composite measure. This composite had a Cronbach's α of 0.75, suggesting good internal consistency.

Neuroimaging Collection and Preprocessing

Participants were scanned at Washington University in St. Louis using a customized Siemens "Connectome" scanner

Table 2. Partial Correlation Results for Application of A Priori Components and De Novo Component

Imaging Modality	Statistic	A Priori HCP_gC1_IC3 Application	A Priori HCP_gC1_IC7 Application	De Novo IC3
Cortical Thickness (sMRI)	*r*	.133	.233[b]	.287[b]
	p	.244	.040	.011
Resting-State Functional Connectivity (rsfcMRI)	*r*	.016	.117[a]	.258[b]
	p	.887	.308	.022
2-Back Working Memory Task (tfMRI)	*r*	.438[c]	.078	.363[c]
	p	<.000	.498	.001

n = 80. All correlations are partial Pearson correlations corrected for group mean differences.

HCP, Human Connectome Project; IC3, independent component 3; sMRI, structural magnetic resonance imaging; tfMRI, task functional magnetic resonance imaging.

[a]For reference, resting-state connectivity data from HCP_gC1_IC7 were not significantly correlated with cognitive control performance in the normative data (33) and thus were not predicted to be significantly correlated with cognitive control in the present dataset. Correlations for a priori ICs are not false discovery rate corrected as we had strong predictions from our prior work that these modalities would predict cognitive control performance in psychosis. The *p* values listed for de novo IC3 are the original uncorrected *p* values; all 3 *p* values meet the false discovery rate–determined critical *p* value of .022.

[b]$p < .05$.

[c]$p < .01$.

(Siemens, Munich, Germany) developed for the HCP (37). T1 and T2 weights were acquired at 0.7 mm isotropic resolution, and blood oxygen level–dependent imaging were collected at 2 mm isotropic resolution with 720-ms repetition time. Data were preprocessed using the HCP pipelines (39) and further processed to generate the final imaging measures used in the present study as was done in (33). Three magnetic resonance imaging (MRI) modalities were used: 1) structural MRI (sMRI) processed for cortical thickness; 2) resting-state functional connectivity (rsfcMRI) correlation matrices generated using cortical (40), cerebellar (41), and subcortical parcels from FreeSurfer (Athinoula A. Martinos Center for Biomedical Imaging, Massachusetts General Hospital, Boston, MA); and, 3) the HCP *n*-back working memory task functional MRI (tfMRI) activation in the 2-back condition (see the Supplement).

Relationship to A Priori Normative Multimodal Correlates of Cognitive Control

Our previous work using mCCA+jICA identified replicable multimodal patterns from 2 mCCA+jICA components that were significantly related to cognitive control in healthy participants in the HCP (33). We performed an analysis to determine whether patterns from these 2 components also predicted cognitive control in the present participants. Given that data were collected and processed identically, we directly applied the 3 relevant modalities from these 2 components from the prior study to the source data from the present cohort (referred to as HCP_gC1_IC3 and HCP_gC1_IC7; see the Supplement). This generated a set of subject-specific weights for the present cohort corresponding to the extent to which a priori components reflected the present data (see the Supplement). Resultant weights were correlated with the composite cognitive control measure.

mCCA+jICA Multimodal Imaging Analysis

We also identified mCCA+jICA components de novo in the psychosis dataset. mCCA+jICA is an unsupervised analysis framework that identifies relationships across modalities and decomposes data to reveal maximally independent latent sources of variance (30,34) (see the Supplement). Briefly, mCCA (42,43) first aligned the 3 imaging modalities to simplify the correlational structure and maximize intersubject covariation (31,33). Next, jICA maximized spatial independence (44), yielding a set of 9 independent components (ICs). Each IC contained a set of three linked imaging modalities; that is, each IC contained a map of cortical thickness (sMRI), a map of working memory task activation (tfMRI), and a parcelwise resting-state correlation matrix (rsfcMRI). Each IC also had a corresponding set of subject-specific weights that reflected the extent to which a given IC composed the participant's original data. These weights were then used for statistical analyses to identify brain-behavior relationships and assess group discriminability (see the Supplement).

Statistical Analyses

Statistical analyses were performed in SPSS, v24 and v25 (IBM Corp., Armonk, NY) and MATLAB R2017a (The MathWorks, Inc., Natick, MA) with multiple comparison correction using false discovery rate (45). For correlations between subject-specific weights and cognitive control performance, partial correlation was used to correct for differences in group means. We assessed group discrimination performance of each IC using multivariate analysis of variance (MANOVA) in which group was used to predict all 3 imaging weights (1 per modality) related to each IC. Significant MANOVA omnibus tests were followed up with planned contrasts.

RESULTS

Behavioral and Demographics

There were no significant group differences in gender, parental education, or socioeconomic status. Groups differed significantly on age, ethnicity, education, symptoms, and cognitive control performance. Participants with SZ had significantly impaired cognitive control performance compared with HC and participants with BD, with no difference between HC and those with BD (Table 1). Dichotomizing participants with BD by psychosis severity revealed that participants with low-psychosis BD performed significantly better than participants with SZ, and those with high-psychosis BD exhibited performance indistinguishable from those with SZ (Supplemental Table S13).

Prediction Using A Priori ICs

Two ICs from Lerman-Sinkoff *et al.* (33) (Supplemental Figures S1and S2) were applied to the present dataset, and resultant weights were partially correlated with cognitive control to identify whether a priori ICs predicted cognitive control in the present dataset (Table 2, Figure 1; Supplemental Figure S3; see the Supplemental Results for individual group correlations). This identified significant predictions from a priori HCP_gC1_IC3

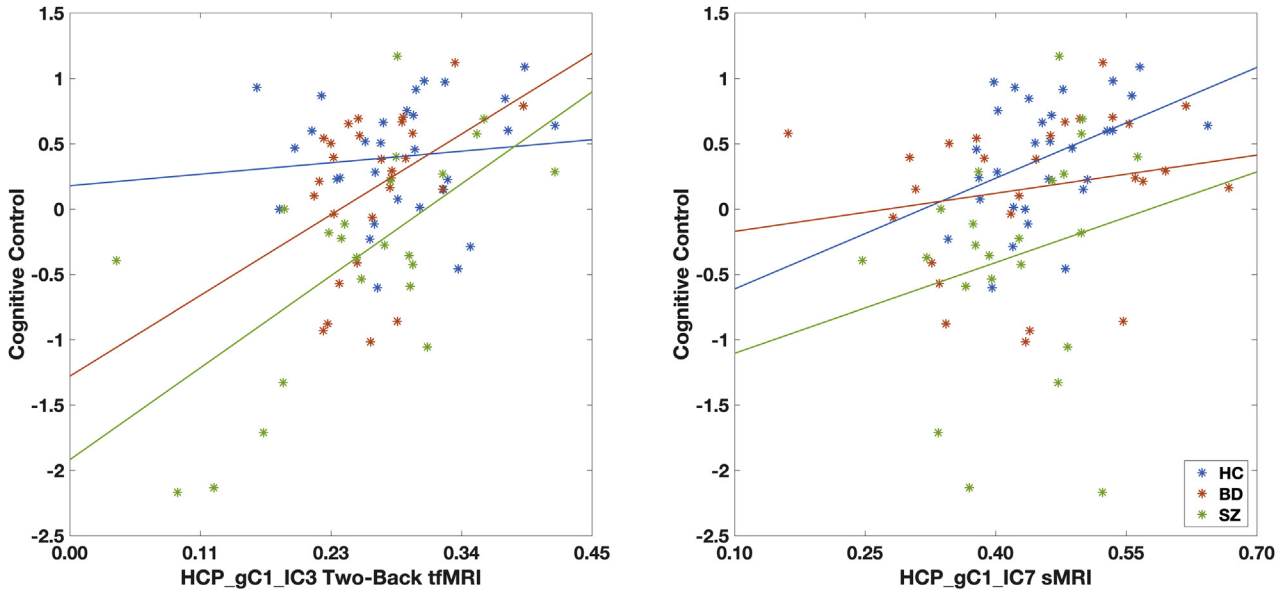

Figure 1. Scatter plots of cognitive control and a priori independent components applied to psychosis cohort. Two of 6 modalities in HCP_gC1_IC3 and HCP_gC1_IC7 significantly predicted cognitive control performance in the psychosis cohort. Scatter plots of the other 4 modalities are available in Supplemental Figure S3. BD, bipolar disorder; HC, healthy control participants; sMRI, structural magnetic resonance imaging; SZ, schizophrenia and schizoaffective disorder; tfMRI, task functional magnetic resonance imaging.

working memory tfMRI and HCP_gC1_IC7 cortical thickness. Follow-up analyses (Figure 1; Supplemental Figure S3, Supplemental Tables S3–S8) identified a significant interaction driven by correlations between these weights and the cognitive control composite for SZ in HCP_gC1_IC3 tfMRI. There were no significant interactions with group for HCP_gC1_IC7 sMRI. Neither HCP_gC1_IC3 nor HCP_gC1_IC7 was group discriminative (Supplemental Tables S16 and S17).

De Novo mCCA+jICA

mCCA+jICA was also performed de novo to identify novel domains of variation in the psychosis cohort. This identified a single component IC3 that significantly correlated with cognitive control for all 3 modalities after false discovery rate correction. Follow-up partial correlations correcting for group were performed, indicating that all 3 modalities still significantly correlated with cognitive control (Table 2). Follow-up analyses (Figure 2; Supplemental Figure S3, Supplemental Tables S9–S11) identified significant interactions in all 3 modalities such that SZ were responsible for the significant correlations between imaging and cognitive control.

Spatial Distributions of De Novo IC3

The modalities in de novo IC3 (Figures 3–5) were visually inspected and bore strong visual resemblances to a priori HCP_gC1_IC3 (Supplemental Figure S1). Algorithmic matching

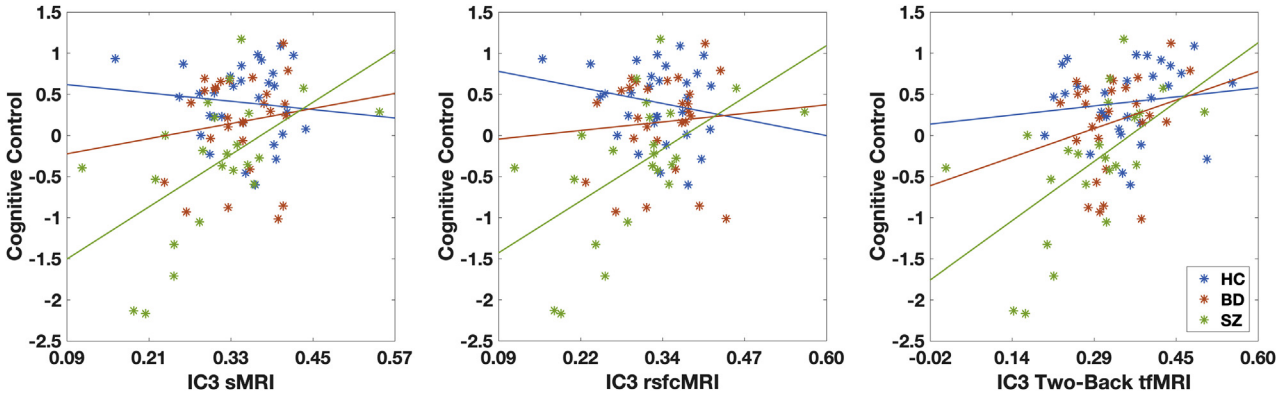

Figure 2. Scatter plots of cognitive control and de novo independent component 3 (IC3) imaging weights. Partial correlations between de novo IC3 imaging weights and cognitive control for all 3 groups pooled were significant for all 3 modalities. Scatter plots by group suggested that this may be driven by participants with schizophrenia and schizoaffective disorder (SZ), which was formally tested using regression analyses (Supplemental Tables S6–S8). BD, bipolar disorder; HC, healthy control participants; rsfcMRI, resting-state functional connectivity magnetic resonance imaging; sMRI, structural magnetic resonance imaging; tfMRI, task functional magnetic resonance imaging.

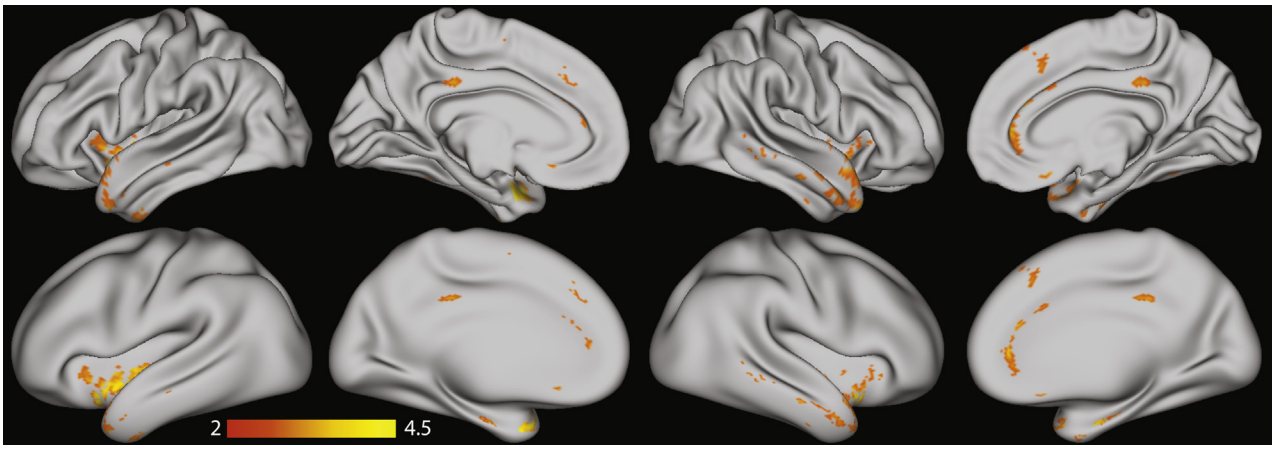

Figure 3. Psychosis independent component (IC) 3–structural magnetic resonance imaging modality. Given that multiset canonical correlation analysis with joint IC analysis generates component maps with a value at every vertex/voxel/pairwise-correlation, maps were thresholded at $|Z| > 2$ to simplify interpretation of the spatial pattern of results in de novo IC3 (31,33). Thus, the maps presented in Figures 3 to 5 and Supplemental Figures S1 and S2 highlight those elements in the map that were strongest relative to all other elements in the given map (unthresholded maps are available in Supplemental Figures S4–S6). (Top) Thresholded IC3 structural magnetic resonance imaging map displayed on the Human Connectome Project HCP Q1-Q6 440 Subject midthickness surface map. (Bottom) Same structural magnetic resonance imaging map displayed on the HCP Q1-Q6 440 Subject inflated surface map.

using η^2 confirmed visual similarity by pairing IC3 with HCP_gC1_IC3 as the strongest match across all ICs with 91.5% shared variance across the 2 ICs (Supplemental Table S1). Matching analyses using individual modalities were also performed (see the Supplement). For sMRI data in IC3 (Figure 3), the strongest positive contributing areas were in bilateral anterior and posterior insula, temporal pole, cingulate, frontal superior cortex, and temporal gyrus. Thus, improved cognitive control performance was related to greater thickness in these areas.

For rsfcMRI data in IC3 (Figure 4), the strongest positive contributions were concentrated in within-network connectivity, the diagonal of the correlation matrix, with improved cognitive control performance related to stronger within-network connectivity. Negative contributions were predominantly concentrated off-diagonal and between the default mode network and the task-positive networks, including the frontoparietal, cingulo-opercular, parietal encoding and retrieval, dorsal attention, and ventral attention networks. Thus, improved cognitive control performance was related to stronger negative connections between networks.

For tfMRI data in IC3 (Figure 5), the strongest positive contributing areas were in bilateral visual cortex, intraparietal sulcus, superior parietal gyrus, precentral sulcus and right middle cingulate, and inferior frontal sulcus, with improved cognitive control performance related to greater activation in these regions. The strongest negative contributions were seen in bilateral isthmus of the cingulate, left supramarginal gyrus, precuneus, and inferior parietal gyrus. Thus, improved cognitive control performance was related to lower activation in these regions.

Group Discrimination

MANOVAs were performed for each IC to assess whether imaging weights were group discriminative. Omnibus MANOVA results were significant with false discovery rate correction only for IC3, the only component significantly related to cognitive control (Table 3); all other ICs were not group discriminative (Supplemental Table S2). Between-subjects effects were significant for tfMRI and trended as significant for sMRI. Post hoc tests between groups were significant for group differences between HC and participants with SZ for sMRI and tfMRI, trend-level significant for differences between participants with BD and SZ for all 3 modalities, and no differences between HC and participants with BD. Although groups did not significantly differ on parental socioeconomic status, inclusion of parental socioeconomic status as a covariate improved the model such that there were trend or significant effects for all modalities (Supplemental Table S9).

DISCUSSION

The goal of the present study was to examine transdiagnostic multimodal neural alterations in psychosis related to cognitive control. Application of a priori ICs identified in the HCP to the psychosis dataset significantly predicted cognitive control performance in a cortical thickness map for all groups and in a working memory map for participants with SZ. De novo mCCA+jICA analysis of the psychosis dataset identified a single IC that significantly correlated with cognitive control performance in participants with SZ. This IC exhibited highly similar spatial distribution to an a priori IC and was the sole group-discriminative IC from the de novo mCCA+jICA results. Importantly, as described below, our multimodal analyses illustrate the ways in which there are both deficits in the same regions and/or networks that cut across modalities, as well as deficits that are modality specific, though contributing to joint prediction of cognitive control. Such results help to link findings in individual modalities of neural structure and/or function into an associated pattern that is correlated with a central domain of cognitive impairment in psychosis.

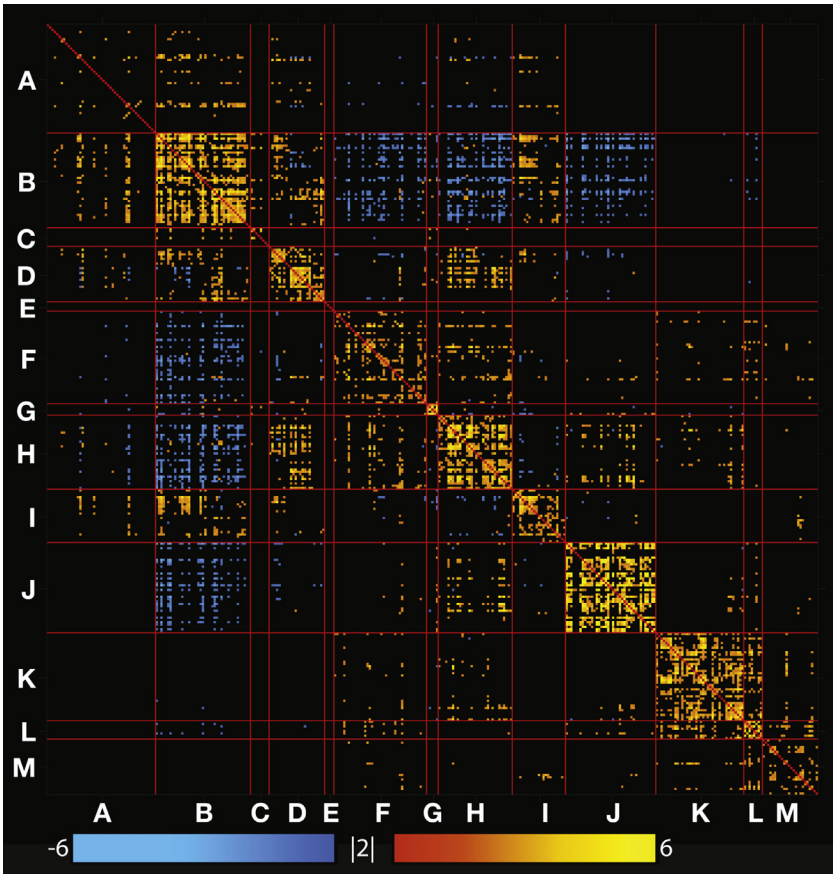

Figure 4. Psychosis independent component 3–resting-state functional connectivity magnetic resonance imaging modality. Resting-state functional connectivity magnetic resonance imaging correlation matrix from psychosis independent component 3, thresholded at $|Z| > 2$ (see Figure 3 for threshold rationale). Network labels: A, none; B, default mode; C, context; D, frontoparietal; E, salience; F, cingulo-opercular; G, parietal encoding and retrieval; H, dorsal attention; I, ventral attention; J, visual; K, somatomotor hand; L, somatomotor mouth; M, auditory.

Our previous multimodal work studying cognitive control in healthy individuals identified a working memory map in HCP_gC1_IC3 that exhibited predominantly posterior cortical contributions in the tfMRI data from the frontoparietal, dorsal attention, and visual networks, which are hypothesized to support rapid-timescale cognitive control functionality (46). It was surprising that this pattern significantly predicted cognitive control in participants with SZ but not BD or in HC, even though it was derived from and significantly correlated with cognitive control in healthy participants in the HCP (see limitations, below). A second component identified in our previous work, HCP_gC1_IC7, contained an sMRI map with positive contributions in the cingulo-opercular, salience, and ventral attention networks and negative contributions in the default mode and visual networks, which are hypothesized to support stable-timescale cognitive control functionality (46). Interestingly, this component significantly predicted cognitive control in the psychosis cohort for all groups. Together, these a priori patterns were partially predictive of cognitive control in the general population as well as in individuals with varying levels of psychosis and may provide clues toward localization of deficits in psychosis.

De novo application of mCCA+jICA to the psychosis dataset identified an IC that was both 91.5% similar to a priori HCP_gC1_IC3 and also significantly correlated with cognitive control performance. However, it was surprising that the de novo correlations with cognitive control were significant only for participants with SZ even though the a priori IC was significant in HC. Thus, we discuss the interpretations of these findings in participants with SZ and address the group specificity of correlations later in the discussion. Nonetheless, the independent identification of 2 highly similar ICs using data-driven methods suggests that these imaging patterns may be robust features in the broader population, though identifying relationships between these patterns and cognitive control performance requires further study.

For tfMRI data, both a priori HCP_gC1_IC3 and de novo IC3 were predictive of cognitive control in participants with SZ. We previously postulated that strong visual contributions may be due to top-down modulation of visual regions, especially given that the working memory tfMRI task was highly visually demanding (47). Independent identification of this pattern de novo may provide intriguing clues toward the source of cognitive control dysfunction in participants with SZ. A number of reports have identified visual system dysfunction in participants with SZ (48–51), though the literature is more mixed for participants with BD (52–57). Theories generated from these lines of research postulate that alterations in visual system functionality lead to aberrant integration of information in higher order cortical areas and lead to dysfunction in cognitive

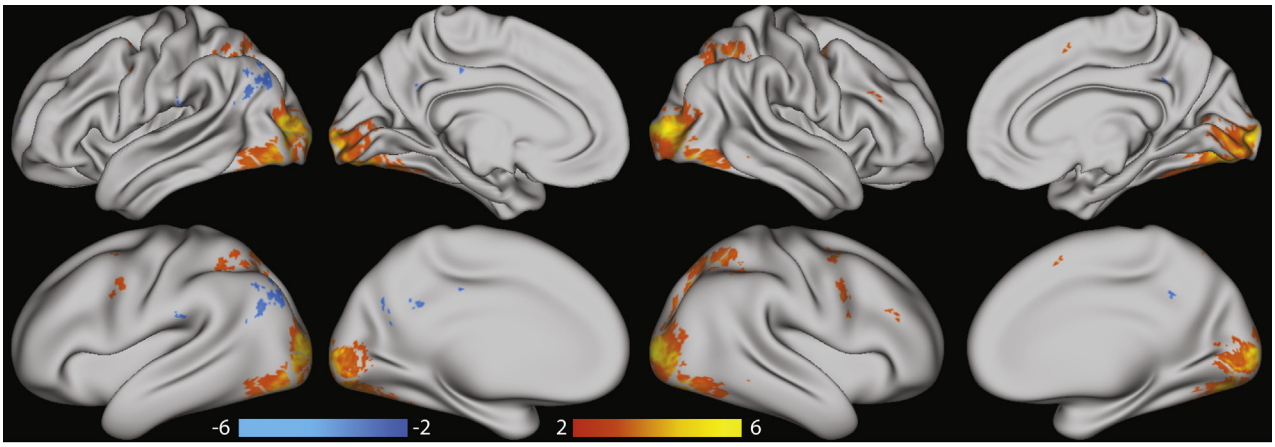

Figure 5. Psychosis independent component 3–working memory task functional magnetic resonance imaging (tfMRI) modality. Working memory tfMRI from psychosis independent component 3, thresholded at $|Z| > 2$ (see Figure 3 for threshold rationale). (Top) Thresholded independent component 3 tfMRI map displayed on the Human Connectome Project HCP Q1-Q6 440 Subject midthickness surface map. (Bottom) Same tfMRI map displayed on the HCP Q1-Q6 440 Subject very inflated surface map.

control (48,51,58). Thus, the present work could be seen as consistent with the hypothesis that impairments in the function and/or structure of the visual cortex may disrupt higher order processing leading to deficits in cognitive control. In the present data, participants with SZ who exhibited greater visual region contributions in IC3 tfMRI data had significantly better cognitive control performance. Importantly, the de novo data for HC and participants with BD trended in the same direction as for participants with SZ, though this trend was not significant (Figure 2). While the present work is not a direct assessment of the relationship between visual system integrity and cognition, the findings are consistent with these models of psychosis in participants with SZ and thus warrant further study.

For sMRI data, de novo IC3 significantly correlated with cognitive control in participants with SZ and exhibited contributions similar to HCP_gC1_IC3 including the insula, medial prefrontal cortex, and cingulate. Transdiagnostic gray matter volume variability has been identified in these regions (21), but relationships with cognitive control in psychosis were not tested. However, Goodkind *et al.* (21) did identify a positive relationship between volume in these regions and cognitive control in HC. Interestingly, small portions of these regions were also present in a priori HCP_gC1_IC7, although contributions were more scattershot, with smaller clusters exceeding the visualization threshold. Importantly, correlations between HCP_gC1_IC7 and cognitive control were significant for all 3 groups. Thus, the data suggest that this finding may

Table 3. IC3 Group-Discrimination MANOVA Results

	Item	Value	Test Statistic	*p* Values	Partial η^2
Omnibus Tests	Pillai's trace	0.219	$F_{6,154} = 3.15$	.006	.109
	Wilk's lambda	0.78	$F_{6,152} = 3.21$	.005	.113
Between-Subjects Effects	sMRI	N/A	$F_{2,78} = 2.52$	.087	.047
	rsfcMRI	N/A	$F_{2,78} = 1.91$	.156	.061
	tfMRI	N/A	$F_{2,78} = 4.59$	.013	.105
	Item	Mean Difference	SE	*p* Values	
Post Hoc Tests	sMRI: HC − BD	0.001	0.018	.936	
	sMRI: HC − SZ	0.038	0.018	.044	
	sMRI: BD − SZ	0.036	0.019	.060	
	rsfcMRI: HC − BD	−0.008	0.019	.679	
	rsfcMRI: HC − SZ	0.030	0.020	.132	
	rsfcMRI: BD − SZ	0.038	0.020	.066	
	tfMRI: HC − BD	0.025	0.022	.255	
	tfMRI: HC − SZ	0.070	0.023	.003	
	tfMRI: BD − SZ	0.045	0.024	.066	

BD, participants with bipolar disorder; HC, healthy control participants; IC, independent component; MANOVA, multivariate analysis of variance; N/A, not applicable; rsfcMRI, resting-state functional connectivity magnetic resonance imaging; sMRI, structural magnetic resonance imaging; SZ, participants with schizophrenia; tfMRI, task functional magnetic resonance imaging.

indeed be transdiagnostic, though further study is clearly warranted.

For rsfcMRI data, de novo IC3 significantly correlated with cognitive control in participants with SZ and exhibited similar contributions to a priori HCP_gC1_IC3. Both a priori HCP_gC1_IC3 and de novo IC3 rsfcMRI maps exhibited modular network structures composed of high within-network connectivity and anticorrelated activity between the task-positive and task-negative networks and resembled a canonical resting-state matrix. Thus, we draw the same general conclusion as in our previous work, namely that there is some evidence that greater presence of canonical resting-state networks may be associated with improved cognitive control.

It was surprising that correlations between imaging and cognitive control were significantly driven by SZ in all analyses except a priori HCP_gC1_IC7 sMRI. This may be due to a variety of factors. First, there was a graded, trend-significant inhomogeneity of variance in cognitive control performance, such that participants with SZ had greater variance than those with BD, who had greater variance than HC. This may have hampered our ability to identify relationships with cognitive control within the other groups. Indeed, for all correlations between imaging and cognitive control (except HCP_gC1_IC7 rsfcMRI, which was not significant in original HCP data), the direction of trend lines was concordant for patients, suggesting the presence of a relationship that we were underpowered to detect. Second, BD inclusion was not limited to individuals with psychosis, and participants with BD endorsed significantly less history of psychotic symptoms than did participants with SZ (Table 1). Importantly, the literature suggests variability in cognitive performance in participants with BD (59), with poorer working memory and executive function performance in participants with psychotic BD, which was also observed in the present study (Supplemental Table S10). Thus, future work with larger BD samples with psychosis are needed to better determine similarity to SZ in multimodal correlates of cognitive control.

There are several additional limitations to the present study. First, de novo mCCA+jICA was a data-driven explorative analysis and must be interpreted with caution. However, given similarity between a priori ICs and the present results, the differences across datasets provide intriguing possibilities for further hypothesis-driven study. Second, the present cognitive control metric was not identical to the HCP metric owing to study design differences, potentially limiting our ability to detect all of the same relationships identified in our previous work (see the Supplement). Third, while IC3 was group discriminative overall, we were unable to detect significant post hoc differences between HC and participants with BD, though differences between HC and participants with SZ were significant and differences between participants with SZ and BD were trend level, which may be due to medications or a relatively unimpaired BD group. Fourth, it was surprising that a priori HCP_gC1_IC3 rsfcMRI did not significantly predict cognitive control in the entire psychosis sample or any of the individual subgroups. This could be due to differences in the behavioral composite across the studies; alternatively, it is possible that the sum of the numerous small but subtle differences in the 2 maps was sufficient to reduce predictive performance. Finally, sample size may have limited our ability to detect group discrimination of a priori ICs, relationships between imaging, and cognitive control, given that we only had behavioral data for 30 HC, 27 participants with BD, and 23 participants with SZ. However, the de novo identification of IC3, which was 91.5% similar to HCP_gC1_IC3, suggests that this pattern is indeed a durable feature in the data and that limited variance in the cognitive control composite was the primary driver of our inability to detect some effects.

In conclusion, the present study employed multimodal methods to examine transdiagnostic alterations in cognitive control in psychosis. Two modalities from a priori ICs from the normative population significantly predicted cognitive control in psychosis for 2 of 6 modalities tested. De novo mCCA+jICA identified a group-discriminative IC that significantly correlated with cognitive control for sMRI, rsfcMRI, and tfMRI data. De novo analyses suggest joint associations between cognitive control and tfMRI contributions from the posterior frontoparietal, dorsal attention, and visual networks; sMRI contributions from the insula, medial PFC, and cingulate; and rsfcMRI contributions from canonical resting-state network organization. However, significant effects were predominantly driven by participants with SZ, with little evidence for effects in participants with BD or HC. Given psychotic symptom heterogeneity in BD, results suggest that shared symptomatology, such as psychosis, may be key to identification of transdiagnostic relationships with cognitive control. Together, these results identified significant and replicable relationships across modalities and the psychosis spectrum, providing targets across modalities of neural structure and function for future research.

ACKNOWLEDGMENTS AND DISCLOSURES

This work was supported by National Institutes of Health (NIH) Medical Scientist Training Program training Grant Nos. 5T32GM007200-38, 5T32GM007200-39 (to DBL-S); Interdisciplinary Training in Cognitive, Computational and Systems Neuroscience Grant No. 5 T32 NS073547-05 (to DBL-S); the McDonnell Center for Systems Neuroscience (to DBL-S); and NIH fellowship Grant No. F30MH109294 (to DBL-S). This work was also supported by National Institute of Mental Health Grant No. R01 MH104414 (to DTM); Taylor Family Institute, Department of Psychiatry (to DTM); and the Center for Brain Research on Mood Disorders, Department of Psychiatry, Washington University Medical School (to DTM). This work was also supported by NIH Grant Nos. 2R01EB006841, 2R01EB005846, and P20GM103472 and National Science Foundation Grant No. 1539067 (to VDC). Computations were performed using the facilities of the Washington University Center for High Performance Computing, which were partially funded by NIH Grant Nos. 1S10RR022984-01A1 and 1S10OD018091-01.

The content of this report is solely the responsibility of the authors and does not necessarily represent the views of the funding agencies.

A version of this manuscript has been posted to the bioRxiv preprint server.

DMB has consulted for Pfizer in the previous 2 years. DBL-S has received payment from an unrelated pharmaceutical company for use of his pet in veterinary product advertisements. All other authors report no other biomedical financial interests or potential conflicts of interest.

ARTICLE INFORMATION

From the Department of Biomedical Engineering (DBL-S), Medical Scientist Training Program (DBL-S), Department of Psychiatry (SK, DMB, DTM), Department of Psychological and Brain Science (DMB), and Department of Radiology (DMB), Washington University in St. Louis, St. Louis, Missouri; Medical Image Analysis Lab (VDC), The Mind Research Network; and Department of Electrical and Computer Engineering (VDC), University of New Mexico, Albuquerque, New Mexico.

Address correspondence to Dov B. Lerman-Sinkoff, B.Sc.E., Washington University in St. Louis, Department of Biomedical Engineering, 1 Brookings Drive, Psych CB 1125, Saint Louis, MO 63130; E-mail: lermand@wustl.edu.

Received Mar 19, 2018; revised Mar 14, 2019; accepted May 1, 2019.

Supplementary material cited in this article is available online at https://doi.org/10.1016/j.bpsc.2019.05.004.

REFERENCES

1. Kapur S (2003): Psychosis as a state of aberrant salience: A framework linking biology, phenomenology, and pharmacology in schizophrenia. Am J Psychiatry 160:13–23.
2. Lewandowski KE, Sperry SH, Cohen BM, Ongür D (2014): Cognitive variability in psychotic disorders: A cross-diagnostic cluster analysis. Psychol Med 44:3239–3248.
3. Barch DM, Ceaser A (2012): Cognition in schizophrenia: Core psychological and neural mechanisms. Trends Cogn Sci 16:27–34.
4. Barch DM, Sheffield JM (2014): Cognitive impairments in psychotic disorders: Common mechanisms and measurement. World Psychiatry 13:224–232.
5. Braver TS, Barch DM, Cohen JD (1999): Cognition and control in schizophrenia: A computational model of dopamine and prefrontal function. Biol Psychiatry 46:312–328.
6. Lesh TA, Niendam TA, Minzenberg MJ, Carter CS (2011): Cognitive control deficits in schizophrenia: Mechanisms and meaning. Neuropsychopharmacology 36:316–338.
7. Smucny J, Lesh TA, Newton K, Niendam TA, Ragland JD, Carter CS (2017): Levels of cognitive control: A functional magnetic resonance imaging-based test of an RDoC domain across bipolar disorder and schizophrenia. Neuropsychopharmacology 154:S1.
8. Bora E, Pantelis C (2015): Meta-analysis of cognitive impairment in first-episode bipolar disorder: Comparison with first-episode schizophrenia and healthy controls. Schizophr Bull 41:1095–1104.
9. McTeague LM, Goodkind MS, Etkin A (2016): Transdiagnostic impairment of cognitive control in mental illness. J Psychiatr Res 83:37–46.
10. Burgess GC, Depue BE, Ruzic L, Willcutt EG, Du YP, Banich MT (2010): Attentional control activation relates to working memory in attention-deficit/hyperactivity disorder. Biol Psychiatry 67:632–640.
11. Cools R, D'Esposito M (2011): Inverted-U-shaped dopamine actions on human working memory and cognitive control. Biol Psychiatry 69:e113–e125.
12. Nigg JT (2017): Annual research review: On the relations among self-regulation, self-control, executive functioning, effortful control, cognitive control, impulsivity, risk-taking, and inhibition for developmental psychopathology. J Child Psychol Psychiatry 58:361–383.
13. Sanislow CA, Pine DS, Quinn KJ, Kozak MJ, Garvey MA, Heinssen RK, *et al.* (2010): Developing constructs for psychopathology research: research domain criteria. J Abnorm Psychol 119:631–639.
14. Botvinick MM, Cohen JD (2014): The computational and neural basis of cognitive control: charted territory and new frontiers. Cogn Sci 38:1249–1285.
15. Botvinick M, Braver T (2015): Motivation and cognitive control: From behavior to neural mechanism. Annu Rev Psychol 66:83–113.
16. Miller EK, Cohen JD (2001): An integrative theory of prefrontal cortex function. Annu Rev Neurosci 24:167–202.
17. Carter CS, Krus MK (2012): Dynamic cognitive control and frontal-cingulate interactions. In: Posner MI, editor. Cognitive Neuroscience of Attention, 2nd ed. New York: Guilford Press, 88–98.
18. Barch DM (2009): Neuropsychological abnormalities in schizophrenia and major mood disorders: Similarities and differences. Curr Psychiatry Rep 11:313–319.
19. Kuswanto C, Chin R, Sum MY, Sengupta S, Fagiolini A, McIntyre RS, *et al.* (2016): Shared and divergent neurocognitive impairments in adult patients with schizophrenia and bipolar disorder: Whither the evidence? Neurosci Biobehav Rev 61:66–89.
20. Hartberg CB, Sundet K, Rimol LM, Haukvik UK, Lange EH, Nesvag R, *et al.* (2011): Brain cortical thickness and surface area correlates of neurocognitive performance in patients with schizophrenia, bipolar disorder, and healthy adults. J Int Neuropsychol Soc 17:1080–1093.
21. Goodkind M, Eickhoff SB, Oathes DJ, Jiang Y, Chang A, Jones-Hagata LB, *et al.* (2015): Identification of a common neurobiological substrate for mental illness. JAMA Psychiatry 72:305–315.
22. Shepherd AM, Quide Y, Laurens KR, O'Reilly N, Rowland JE, Mitchell PB, *et al.* (2015): Shared intermediate phenotypes for schizophrenia and bipolar disorder: Neuroanatomical features of subtypes distinguished by executive dysfunction. J Psychiatry Neurosci 40:58–68.
23. Du Y, Pearlson GD, Lin D, Sui J, Chen J, Salman M, *et al.* (2017): Identifying dynamic functional connectivity biomarkers using GIG-ICA: Application to schizophrenia, schizoaffective disorder, and psychotic bipolar disorder. Hum Brain Mapp 38:2683–2708.
24. Du Y, Pearlson GD, Liu J, Sui J, Yu Q, He H, *et al.* (2015): A group ICA based framework for evaluating resting fMRI markers when disease categories are unclear: Application to schizophrenia, bipolar, and schizoaffective disorders. Neuroimage 122:272–280.
25. Argyelan M, Ikuta T, DeRosse P, Braga RJ, Burdick KE, John M, *et al.* (2014): Resting-state fMRI connectivity impairment in schizophrenia and bipolar disorder. Schizophr Bull 40:100–110.
26. Sheffield JM, Kandala S, Tamminga CA, Pearlson GD, Keshavan MS, Sweeney JA, *et al.* (2017): Transdiagnostic associations between functional brain network integrity and cognition. JAMA Psychiatry 74:605–613.
27. Meda SA, Gill A, Stevens MC, Lorenzoni RP, Glahn DC, Calhoun VD, *et al.* (2012): Differences in resting-state functional magnetic resonance imaging functional network connectivity between schizophrenia and psychotic bipolar probands and their unaffected first-degree relatives. Biol Psychiatry 71:881–889.
28. Meda SA, Clementz BA, Sweeney JA, Keshavan MS, Tamminga CA, Ivleva EI, *et al.* (2016): Examining functional resting-state connectivity in psychosis and its subgroups in the bipolar-schizophrenia network on intermediate phenotypes cohort. Biol Psychiatry Cogn Neurosci Neuroimaging 1:488–497.
29. Brandt CL, Eichele T, Melle I, Sundet K, Server A, Agartz I, *et al.* (2014): Working memory networks and activation patterns in schizophrenia and bipolar disorder: Comparison with healthy controls. Br J Psychiatry 204:290–298.
30. Calhoun VD, Sui J (2016): Multimodal fusion of brain imaging data: A key to finding the missing link(s) in complex mental illness. Biol Psychiatry Cogn Neurosci Neuroimaging 1:230–244.
31. Sui J, Pearlson GD, Du Y, Yu Q, Jones TR, Chen J, *et al.* (2015): In search of multimodal neuroimaging biomarkers of cognitive deficits in schizophrenia. Biol Psychiatry 78:794–804.
32. Doan NT, Kaufmann T, Bettella F, Jørgensen KN, Brandt CL, Moberget T, *et al.* (2017): Distinct multivariate brain morphological patterns and their added predictive value with cognitive and polygenic risk scores in mental disorders. Neuroimage Clin 15:719–731.
33. Lerman-Sinkoff DB, Sui J, Rachakonda S, Kandala S, Calhoun VD, Barch DM (2017): Multimodal neural correlates of cognitive control in the Human Connectome Project. Neuroimage 163:41–54.
34. Sui J, Adali T, Yu Q, Chen J, Calhoun VD (2012): A review of multivariate methods for multimodal fusion of brain imaging data. J Neurosci Methods 204:68–81.
35. Sui J, He H, Liu J, Yu Q, Adali T, Pearlson GD, *et al.* (2012): Three-way FMRI-DTI-methylation data fusion based on mCCA+jICA and its application to schizophrenia. Conf Proc IEEE Eng Med Biol Soc 2012: 2692–2695.
36. Sui J, Pearlson G, Caprihan A, Adali T, Kiehl KA, Liu J, *et al.* (2011): Discriminating schizophrenia and bipolar disorder by fusing fMRI and DTI in a multimodal CCA+ joint ICA model. Neuroimage 57:839–855.
37. Van Essen DC, Smith SM, Barch DM, Behrens TE, Yacoub E, Ugurbil K, *et al.* (2013): The WU-Minn Human Connectome Project: An overview. Neuroimage 80:62–79.
38. Gur RC, Richard J, Hughett P, Calkins ME, Macy L, Bilker WB, *et al.* (2010): A cognitive neuroscience-based computerized battery for efficient measurement of individual differences: Standardization and initial construct validation. J Neurosci Methods 187:254–262.

39. Glasser MF, Sotiropoulos SN, Wilson JA, Coalson TS, Fischl B, Andersson JL, *et al.* (2013): The minimal preprocessing pipelines for the Human Connectome Project. Neuroimage 80:105–124.
40. Gordon EM, Laumann TO, Adeyemo B, Huckins JF, Kelley WM, Petersen SE (2016): Generation and evaluation of a cortical area parcellation from resting-state correlations. Cereb Cortex 26:288–303.
41. Culbreth AJ, Kandala S, Markow Z, Barch DM (2016): Cerebellar Connectivity and Psychotic-Like Experiences. Atlanta, GA: Society for Biological Psychiatry.
42. Correa NM, Li YO, Adali T, Calhoun VD (2008): Canonical correlation analysis for feature-based fusion of biomedical imaging modalities and its application to detection of associative networks in schizophrenia. IEEE J Sel Top Signal Process 2:998–1007.
43. Li Y-O, Adalı T, Wang W, Calhoun VD (2009): Joint blind source separation by multi-set canonical correlation analysis. IEEE Trans Signal Process 57:3918–3929.
44. Calhoun VD, Adali T, Kiehl KA, Astur R, Pekar JJ, Pearlson GD (2006): A method for multitask fMRI data fusion applied to schizophrenia. Hum Brain Mapp 27:598–610.
45. Benjamini Y, Hochberg Y (1995): Controlling the false discovery rate: A practical and powerful approach to multiple testing. J Roy Stat Soc Ser B (Methodol) 57:289–300.
46. Dosenbach NU, Fair DA, Miezin FM, Cohen AL, Wenger KK, Dosenbach RA, *et al.* (2007): Distinct brain networks for adaptive and stable task control in humans. Proc Natl Acad Sci U S A 104:11073–11078.
47. Barch DM, Burgess GC, Harms MP, Petersen SE, Schlaggar BL, Corbetta M, *et al.* (2013): Function in the human connectome: Task-fMRI and individual differences in behavior. Neuroimage 80:169–189.
48. Silverstein S, Keane BP, Blake R, Giersch A, Green M, Keri S (2015): Vision in schizophrenia: Why it matters. Front Psychol 6:709.
49. Silverstein SM (2016): Visual perception disturbances in schizophrenia: A unified model. In: Silverstein SM, editor. The Neuropsychopathology of Schizophrenia: Molecules, Brain Systems, Motivation, and Cognition, 3rd ed. Cham, Switzerland: Springer International Publishing, 77–132.
50. Yoon JH, Sheremata SL, Rokem A, Silver MA (2013): Windows to the soul: Vision science as a tool for studying biological mechanisms of information processing deficits in schizophrenia. Front Psychol 4:681.
51. Javitt DC (2009): When doors of perception close: Bottom-up models of disrupted cognition in schizophrenia. Annu Rev Clin Psychol 5:249–275.
52. Chen Y, Levy DL, Sheremata S, Holzman PS (2006): Bipolar and schizophrenic patients differ in patterns of visual motion discrimination. Schizophr Res 88:208–216.
53. Chen Y, Bidwell LC, Holzman PS (2005): Visual motion integration in schizophrenia patients, their first-degree relatives, and patients with bipolar disorder. Schizophr Res 74:271–281.
54. Yeap S, Kelly SP, Reilly RB, Thakore JH, Foxe JJ (2009): Visual sensory processing deficits in patients with bipolar disorder revealed through high-density electrical mapping. J Psychiatry Neurosci 34:459–464.
55. Jahshan C, Wynn JK, McCleery A, Glahn DC, Altshuler LL, Green MF (2014): Cross-diagnostic comparison of visual processing in bipolar disorder and schizophrenia. J Psychiatr Res 51:42–48.
56. Maekawa T, Katsuki S, Kishimoto J, Onitsuka T, Ogata K, Yamasaki T, *et al.* (2013): Altered visual information processing systems in bipolar disorder: Evidence from visual MMN and P3. Front Hum Neurosci 7:403.
57. VanMeerten NJ, Dubke RE, Stanwyck JJ, Kang SS, Sponheim SR (2016): Abnormal early brain responses during visual search are evident in schizophrenia but not bipolar affective disorder. Schizophr Res 170:102–108.
58. Phillips WA, Silverstein SM (2013): The coherent organization of mental life depends on mechanisms for context-sensitive gain-control that are impaired in schizophrenia. Front Psychol 4:307.
59. Bora E (2018): Neurocognitive features in clinical subgroups of bipolar disorder: A meta-analysis. J Affect Disord 229:125–134.